J Solid State Electrochem (2009) 13:391–395
DOI 10.1007/s10008-008-0572-9

ORIGINAL PAPER

Evaluation of $La_{0.5}Sr_{0.5}FeO_{3-\delta}$ membrane reactors for partial oxidation of methane

Victor L. Kozhevnikov · Ilia A. Leonidov · Mikhail V. Patrakeev · Alexey A. Markov · Yakov N. Blinovskov

Received: 20 March 2008 / Revised: 23 April 2008 / Accepted: 24 April 2008 / Published online: 27 May 2008

Abstract Dense planar and tubular oxygen separation membranes of $La_{0.5}Sr_{0.5}FeO_{3-\delta}$ were studied in the partial oxidation of methane to syngas process. The oxygen permeation properties were obtained from the analysis of the outlet gas and compared with the data calculated from conductivity measurements. For the planar reactor, the selectivity achieved 95% and the CH_4 conversion was 95–99% at 900 °C with pure methane. For the tubular reactor, the CO selectivity and CH_4 conversion were 90% and 100%, respectively, under the same conditions. In both cases, the H_2/CO ratio was 1.6–1.9. No degradation of membranes was observed after 250 h of operation.

Keywords Mixed conductors · Oxygen permeation · Ceramic membrane · Partial oxidation of methane · Selectivity

Introduction

Though the idea of partial oxidation of methane (POM) in syngas (mixture of CO and H_2) in a membrane reactor utilizing conducting properties of oxides is suggested quite a while ago, it has not been introduced into the practice yet because of the difficulties related to the invention of mixed, oxygen ion and electron, conductors (MIECs) having sufficiently large ambipolar conductivity and simultaneously exhibiting structural and dimensional stability under conditions of the POM process. A number of MIECs have been tested in POM reactors [1–7]. Particularly promising results have been obtained with the use of perovskite-like oxides (or their derivatives) containing cobalt [2, 5]. Unfortunately, the conducting and oxygen-separating properties of cobaltites degrade fairly fast under the harsh conditions of the POM process because of the reduction of cobalt species [8] followed by the loss of structural integrity of membranes. The ferrous materials like, e.g., $(La,Sr)FeO_{3-\delta}$, exhibit higher thermodynamic stability than cobaltites and, therefore, seem to be more suitable for the POM reactor [9]. Moreover, the dimensional changes in ferrites with temperature and oxygen content variations are generally smaller than in cobaltites [10, 11]. The maximum value for ambipolar conductivity in the $(La,Sr)FeO_{3-\delta}$ system is achieved when concentration of lanthanum is equal to that of strontium [12]. In this work, we have studied the functioning of the planar and tubular POM reactors with oxygen-separating membranes made of $La_{0.5}Sr_{0.5}FeO_{3-\delta}$.

Experimental

The ferrite powder was prepared via the glycine–nitrate process, a self-combustion method using glycine as fuel and nitrates of the metal components as the oxidant [13]. This powder was used to press thin pellets under 200 MPa of uniaxial pressure. The pellets were sintered in air at 1,300 °C to produce gas-impervious ceramic membranes. The hydrostatic weighing was employed for the estimation the density of ceramics that consisted not lower then 93%. To obtain tubular membranes, the ferrite powder was mixed with wax and extruded with the help of a Haake PolyDrive extruder. After removing the organic binder at moderate heating, the membranes were sintered in air. The density of the membranes was about 95% of theoretical. The X-ray

V. L. Kozhevnikov (✉) · I. A. Leonidov · M. V. Patrakeev (✉) · A. A. Markov · Y. N. Blinovskov
Institute of Solid State Chemistry, Ural Branch of RAS,
91 Pervomaiskaya Str.,
Yekaterinburg, Russia
e-mail: kozhevnikov@ihim.uran.ru

diffraction analysis of the sintered membranes showed formation of the single-phase rhombohedral $La_{0.5}Sr_{0.5}FeO_{3-\delta}$ with the crystal lattice parameters a=5.502(2) and c= 13.418(5) Å (in a hexagonal setting).

The sketch of the experimental setup is shown in Fig. 1. The gas treatment was carried out with the help of a unified gas preparation system (GPS) equipped with digital mass flow controllers Bronkhorst (MFC). The GPS enabled one to mix Ar and CH_4 in desirable proportions and to vary the flow of the mixture from 2 to 100 ml/min. The pump served to flush the "high pressure" side of the oxygen membrane with air. The outlet gas was dried in a condenser and analyzed with the using of a Crystal 2000M chromatograph (gas chromatography, GC). The experimental parameters were controlled and changed with a personal computer. The planar reactor included a pellet-like planar MIEC membrane with the thickness of 1.5–2 mm. The membrane diameter was 20 mm. The membrane separated gas compartments attached to the feed pipes. The specially prepared glass (GS) was used for sealing the membrane. The catalyst was made of porous Al_2O_3 granules with the average size of about 2 mm and loaded with 10 wt% of nickel. The 10-mm-thick catalytic bed was placed atop the MIEC membrane.

The tubular reactor utilized the MIEC membrane with the length of 50 mm. The membrane diameter was 9 mm; the wall thickness was 0.9 mm. The alumina auxiliary tubes were used to set the MIEC tubular membrane in the hot zone of the electrical furnace. The GS gaskets were used for sealing. The air was pumped inside the membrane. The space between the membrane and quartz-isolating cover, where mixtures of argon with methane or pure methane were fed, was filled with the Ni/Al_2O_3 catalyst.

Results and discussion

Definitions and estimates of oxygen permeability

To evaluate the performance of the membrane, we used the oxygen permeability calculated from the conductivity measurements. The conductivity data depending on temperature and oxygen partial pressure were approximated with the known expression for mixed conductors

$$\sigma(T,p_{O_2}) = \sigma_i + \sigma_p^o p_{O_2}^{+1/4} + \sigma_n^o p_{O_2}^{-1/4} \quad (1)$$

where parameters σ_i,σ_p^o, and σ_n^o were taken from [12]. Assuming diffusion-controlled transport, the oxygen flux density through the MIEC membrane with the thickness of L was calculated from Wagner's equation

$$J_{O_2} = -\frac{RT}{16F^2L}\int_{\ln p_{O2}^{high}}^{\ln p_{O2}^{low}} \frac{\sigma_i\sigma_{el}}{\sigma_i+\sigma_{el}} d\ln p_{O_2} \quad (2)$$

where $p_{O_2}^{low}$ and $p_{O_2}^{high}$ designate values of oxygen partial pressure at the membrane sides flushed by methane and air, respectively, and σ_{el} is the sum of contributions to

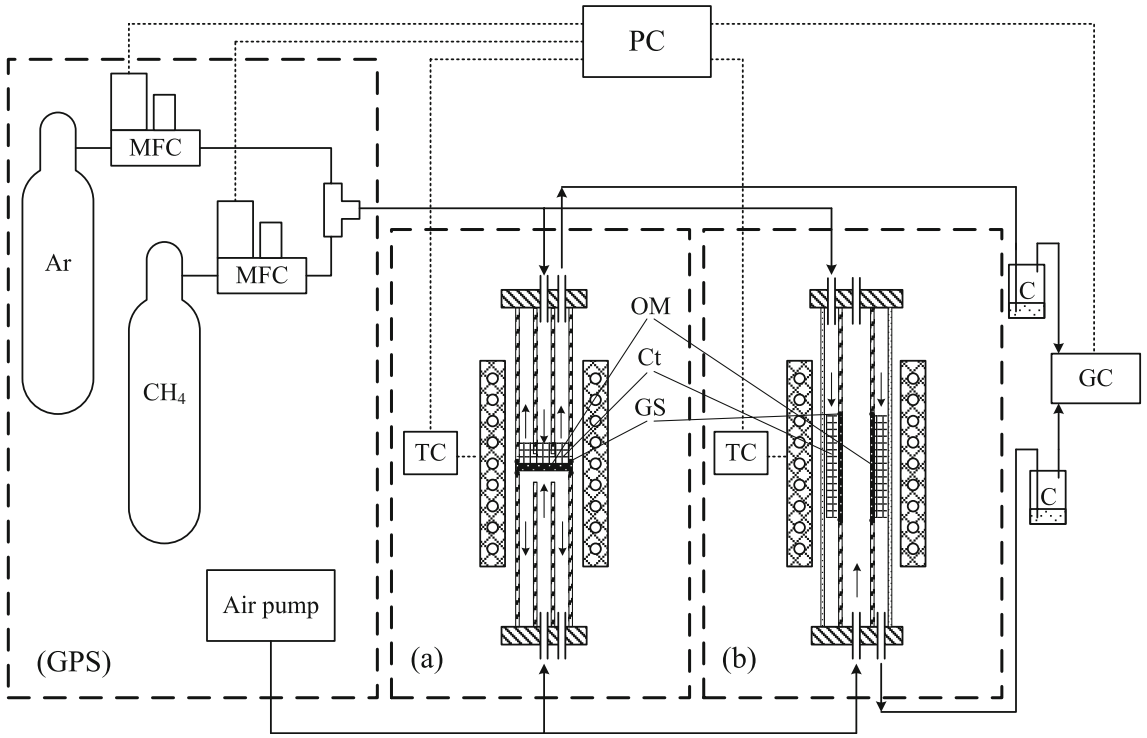

Fig. 1 The sketch of the experimental setup

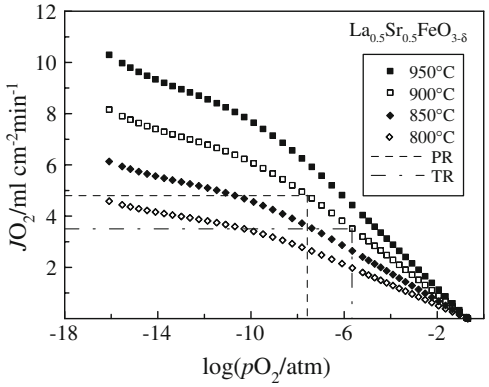

Fig. 2 The oxygen permeation for the 1-mm-thick membrane of $La_{0.5}Sr_{0.5}FeO_{3-\delta}$ depending on the oxygen pressure at the permeate side. The other side of the membrane is exposed to air. *PR* and *TR* are achieved flux densities in planar and tubular reactors, respectively

conductivity from electron and hole carriers. The results calculated at 800–950 °C are shown in Fig. 2 where it is seen that the oxygen flux density achieves 10 ml/(min·cm^2) at 950 °C and $p_{O_2}^{low}=10^{-16}$ atm. From thermodynamic consideration, it follows that the full conversion of methane at 950 °C and $p_{O_2}^{low}=10^{-16}$ atm should result in the gas phase that contains products of partial oxidation and combustion in the volume ratio $H_2/CO/H_2O/CO_2$=40:24:26:10, while the selectivity for CO should be about 70%.

The test conditions were selected to prevent soot formation. The performance of the reactor under tests was evaluated on the basis of the outlet gas composition and material balance. The methane conversion was defined as

$$X_{CH_4}=\left(\frac{v_{CO}+v_{CO_2}}{v_{CH_4}^{outlet}+v_{CO}+v_{CO_2}}\right)\times 100\% \quad (3)$$

where v_i is the volume fraction of species i. The selectivity for CO was calculated as

$$S_{CO}=\left(\frac{v_{CO}}{v_{CO}+v_{CO_2}}\right)\times 100\% \quad (4)$$

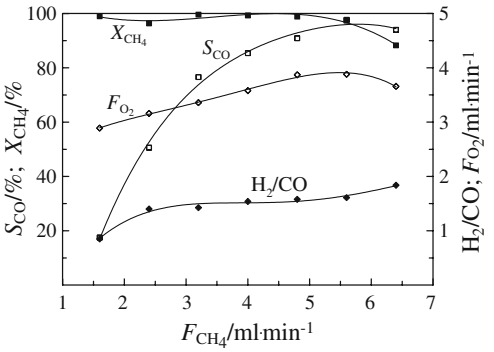

Fig. 3 The performance characteristics for the planar reactor at 900 °

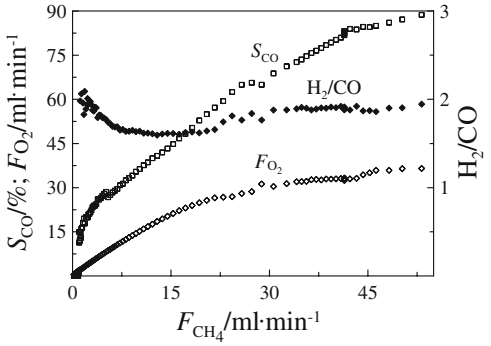

Fig. 4 The performance characteristics for the tubular reactor at 900 °C

The carbon balance was found from

$$B=F\times\frac{v_{CH_4}^{outlet}+v_{CO}+v_{CO_2}}{v_{CH_4}^{inlet}} \quad (5)$$

where F is the total outlet flux of dehumidified gases. The flow of oxygen through the membrane under test was obtained from the outlet gas composition [14] according to

$$F_{O_2}^{perm}=F\times\left(2v_{CO_2}+1.5v_{CO}-0.5v_{H_2}-\frac{0.21}{0.78}\sqrt{\frac{28}{32}}\times v_{N_2}\right) \quad (6)$$

Planar reactor

The reactor was equipped with the 1.9-mm-thick membrane and sealed. The free surface of the membrane was 1.6 cm^2. The feed Ar/CH_4 mixture contained 10% of methane. The starting amount of the inlet gas was 2 ml/min. This stage served to equilibrate the membrane with the ambient gas phase and to activate the catalyst; the selectivity for CO approached 20%, while the ratio H_2/CO was near unity. The appearance of about 0.5% C2 hydrocarbons was registered during the starting period in the outlet stream of both planar and tubular reactors, while at high selectivity,

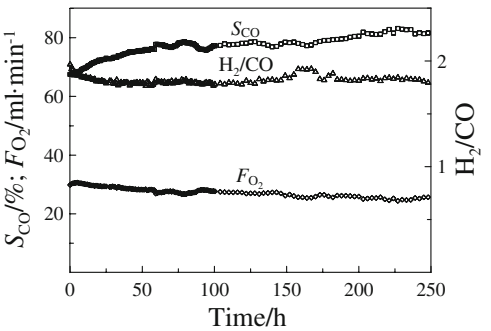

Fig. 5 The performance characteristics of the time-depending test for the tubular reactor at 900 °C

concentrations of these products were below the detection level. The carbon balance was 1±0.03. The Ar content in the feed gas was gradually decreased to zero, and pure methane was let in the reactor. The changes in conversion, selectivity, oxygen flow, and the H_2/CO ratio depending on the methane flow are shown in Fig. 3. It is seen that the selectivity for CO grows up with the increase in the methane feed and attains nearly 95% at F_{CH_4}=5.5 ml/min, whereas the methane conversion just slightly varies within 95–99%. The oxygen permeation flux density across the standard 1-mm-thick membrane at 900 °C achieves 4.6–4.8 ml/(min·cm^2), which is about 60% of the flux density calculated from the partial components of electrical conductivity (Fig. 2). The smaller value can be explained, for instance, by sluggish surface exchange kinetics [6]. It seems, however, that the major reason for this difference is in the oxygen activity gradient across the membrane smaller under conditions of the real POM process than the gradient used in the calculations with Eq. 2. Indeed, the experimentally observed oxygen flux density is expected to be achieved at a rather large oxygen partial pressure, $pO_2^{low}=10^{-7}$ atm, near the membrane side flushed by methane. Therefore, special efforts should be taken to support much lower oxygen activity at the "low pressure" side and to provide larger values of the permeate oxygen flux density.

Further increase in the methane feed resulted in decrease in the methane conversion and in the growth of the H_2/CO ratio to 1.9. In addition, a small amount of methane was detected in the outlet. The total time of the experiment was 250 h. The concentration of nitrogen in the outlet gas did not exceed 1%. No degradation of the membrane was noticeable during the experiment.

Tubular reactor

The startup of the reactor and activation of the catalysts were carried out as described above. The concentration of nitrogen in the outlet gas did not exceed 0.1% after sealing. The concentration of argon in the inlet gas was gradually decreased to zero, and pure methane was let in the reactor when the total inlet gas flow achieved 20 cm^3/min. The data characterizing the performance of the tubular membrane are shown in Fig. 4. The reactor design ensured 100% methane conversion. The oxygen permeation flow through the membrane was observed to increase to 38 ml/min in accord with the increase in the methane feed. The selectivity S_{CO} achieved about 90% at F_{CH_4}=50 ml/min. The H_2/CO ratio was sensitive to the composition and volume flow of the inlet gas. The increased values for H_2/CO at small methane flows are related to uncertainties in GC determination of the CO content in the outlet gas. With larger methane flow, 50 ml/min, the H_2/CO ratio was stably near 1.9.

With the oxygen flow of 38 ml/min, the average oxygen permeation flux density $J(O_2)$ was 3.5 ml/(min·cm^2), i.e., smaller than that calculated from conductivity. As in the case of the planar membrane, the insufficiently large gradient of oxygen activity across the membrane seems to result in this difference. It is possible also that the nonuniform distribution of oxygen activity along the membrane at the permeate side adds to the further decline of the membrane performance. It is seen from Fig. 4 that the oxygen permeate flow does not change significantly at F_{CH_4}>30 ml/min. Therefore, a performance test depending on time was carried out at F_{CH_4}=30 ml/min (Fig. 5). The total test time was 250 h. The selectivity slightly increased while oxygen flow decreased with time. The H_2/CO ratio was about 1.8. After the reactor was stopped, the X-ray diffraction study of membrane was carried out. No changes in the phase composition of the membrane were found. However, the catalyst crumbling was observed to a certain extent.

Conclusion

The ferrous oxide $La_{0.5}Sr_{0.5}FeO_{3-\delta}$ was tested as a membrane material in POM reactors with planar and tubular designs. High values were obtained for CO selectivity and CH_4 conversion. The observed oxygen permeation flux densities achieved 40–60% of the densities calculated from conductivity data. The deviations are believed to be mostly related to the distribution of the oxygen activity gradient across membranes, and hence, they can be reduced by changing the reactor design. The inspection of the reactor materials after test runs revealed some deterioration of Ni/Al_2O_3 catalysts while no signs of degradation of the membrane materials were detected.

Acknowledgements Authors are grateful to the National Innovation Company "New Energy Projects" for the support of this work.

References

1. Balachandran V, Dusek JT, Mieville RL, Poeppel RB, Kleefisch MS, Pei S, Kobylinski TP, Udovich CA, Bose AC (1995) Appl Catal A 133:19
2. Tsai C, Dixon AG, Moser WR, Ma YH (1997) AIChE J 43:2741
3. Mazanec TJ (1997) Electropox gas reforming. In: Anderson HU, Khandar AC, Liu M (eds) Ceramic membranes I. PV95-24. The Electrochemical Society, Penington, NJ, pp 16–28
4. Sammells AF, Schwarz M, Mackay RA, Barton NF, Peterson DR (2000) Catal Today 56:325
5. Dong H, Shao ZP, Xiong GX, Tong JH, Sheng SS, Yang WS (2001) Catal Today 67:3
6. Bouwmeester HJM (2003) Catal Today 82:141
7. Diethelm S, Sfeir J, Clemens F, van Herle J, Favrat D (2004) J Solid State Electrochem 8:611
8. Zhu X, Wang H, Cong Y, Yang W (2006) Catal Letters 111:179

9. Patrakeev MV, Leonidov IA, Kozhevnikov VL, Kharton VV (2004) Solid State Sci 6:907
10. Kharton VV, Shaula AL, Snijkers FMM, Cooymans JFC, Luyten JJ, Marozau IP, Viskup AP, Marques FMB, Frade JR (2006) J Europ Ceram Soc 26:3695
11. Tai L-V, Nasrallah MM, Anderson HU, Sparlin DM, Sehlin SR (1995) Solid State Ionics 76:259
12. Patrakeev MV, Bahteeva JA, Mitberg EB, Leonidov IA, Kozhevnikov VL, Poeppelmeier KR (2003) Solid State Chem 172:1
13. Chick LA, Pederson LR, Maupin GD, Bates JL, Thomas LE, Exarhos GL (1990) Mater Lett 10:6
14. Hu J, Xing T, Jia Q, Hao H, Yang D, Guo Y, Hu X (2006) Appl Catal A 306:29